Neto proteins regulate gating of the kainate-type glutamate receptor GluK2 through two binding sites

Received for publication, March 28, 2019, and in revised form, October 15, 2019 Published, Papers in Press, October 18, 2019, DOI 10.1074/jbc.RA119.008631

Yan-Jun Li[‡1], Gui-Fang Duan[‡1], Jia-Hui Sun[‡1], Dan Wu[‡], Chang Ye[‡], Yan-Yu Zang[‡], Gui-Quan Chen[‡§], Yong-Yun Shi[¶], Jun Wang[‖], Wei Zhang[2], and Yun Stone Shi[‡§‡‡3]**

*From the [‡]State Key Laboratory of Pharmaceutical Biotechnology, Department of Neurology, Affiliated Drum Tower Hospital of Nanjing University Medical School, and Ministry of Education Key Laboratory of Model Animal for Disease Study, Model Animal Research Center, the [§]Institute for Brain Sciences, and the [‡‡]Chemistry and Biomedicine Innovation Center, Nanjing University, Nanjing 210032, the [¶]Department of Orthopaedics, Luhe People's Hospital Affiliated to Yangzhou University, Nanjing 211500, the [‖]Ministry of Education Key Laboratory of Modern Toxicology, Department of Toxicology, School of Public Health, Nanjing Medical University, Nanjing 211166, and the **Institute of Chinese Integrative Medicine, Hebei Medical University, Shijiazhuang 050017, China*

Edited by Roger J. Colbran

The neuropilin and tolloid-like (Neto) proteins Neto1 and Neto2 are auxiliary subunits of kainate-type glutamate receptors (KARs) that regulate KAR trafficking and gating. However, how Netos bind and regulate the biophysical functions of KARs remains unclear. Here, we found that the N-terminal domain (NTD) of glutamate receptor ionotropic kainate 2 (GluK2) binds the first complement C1r/C1s-Uegf-BMP (CUB) domain of Neto proteins (*i.e.* NTD-CUB1 interaction) and that the core of GluK2 (GluK2ΔNTD) binds Netos through domains other than CUB1s (core-Neto interaction). Using electrophysiological analysis in HEK293T cells, we examined the effects of these interactions on GluK2 gating, including deactivation, desensitization, and recovery from desensitization. We found that NTD deletion does not affect GluK2 fast gating kinetics, the desensitization, and the deactivation. We also observed that Neto1 and Neto2 differentially regulate GluK2 fast gating kinetics, which largely rely on the NTD-CUB1 interactions. NTD removal facilitated GluK2 recovery from desensitization, indicating that the NTD stabilizes the GluK2 desensitization state. Co-expression with Neto1 or Neto2 also accelerated GluK2 recovery from desensitization, which fully relied on the NTD-CUB1 interactions. Moreover, we demonstrate that the NTD-CUB1 interaction involves electric attraction between positively charged residues in the GluK2_NTD and negatively charged ones in the CUB1 domains. Neutralization of these charges eliminated the regulatory effects of the NTD-CUB1 interaction on GluK2 gating. We conclude that KARs bind Netos through at least two sites and that the NTD-CUB1 interaction critically regulates Neto-mediated GluK2 gating.

In the central nervous system, excitatory synaptic transmission is primarily mediated by glutamate. Glutamate released from presynaptic terminals excites three types of ionotropic glutamate receptors, which are pharmacologically classified as AMPA[4] (amino-3-hydroxy-5-methylisoxazole-4-propionic acid) receptors (AMPARs), NMDA (*N*-methyl-D-aspartic acid) receptors (NMDARs), and kainate receptors (KARs) (1). AMPARs mediate the majority of fast transmission, whereas NMDARs are responsible for synaptic plasticity. KARs are expressed in subsets of neuronal types in the brain. They not only contribute to excitatory postsynaptic currents on postsynaptic cells; they also regulate neurotransmitter release on the presynaptic terminal (2). Additionally, KAR activity is involved in synaptic plasticity (3). Dysfunction of KARs causes neurologic diseases such as epilepsy, schizophrenia, and autism (2, 4).

Ionotropic glutamate receptors are tetramers. Each subunit contains a large N-terminal domain (NTD), accounting for about 40% of the full length, followed by a ligand-binding domain (LBD) and a transmembrane domain (TMD) forming the ion channel pore and then an intracellular C-terminal tail associating with scaffold proteins. Among these domains, the NTD is the largest, but its function, until recently, has been poorly understood. The NTDs of NMDARs are important for their gating and regulation by allosteric modulators, including Zn^{2+}, H^+, ifenprodil, etc. (1, 5, 6). The NTDs of AMPARs play little role in receptor fast gating but instead contribute to the stabilization of desensitization (7). Additionally, NTD-truncated AMPAR subunits display increased mobility on synapse and lose their ability to sustain long-term potentiation (8, 9). Similar to AMPARs, removal of GluK2_NTD does not change the rates of deactivation and desensitization in heterologous systems (10), whereas NTDs of KARs are crucial for synaptic localization (11, 12).

This work is supported by National Natural Science Foundation of China Grants 91849112, 31571060, 81573416, and 31371061 (to W. Z. and Y. S. S.); Basic Research Program of Jiangsu Province Grant BE2019707 (to Y. S. S.); Outstanding Youth Foundation of Jiangsu Province of China Grant BK20140018 (to Y. S. S.); and Fundamental Research Funds for the Central Universities Grant 0903-14380029. The authors declare that they have no conflicts of interest with the contents of this article.

This article contains Figs. S1–S5.

[1] These authors contributed equally to this work.

[2] To whom correspondence may be addressed. E-mail: weizhang@hebmu.edu.cn.

[3] To whom correspondence may be addressed. E-mail: yunshi@nju.edu.cn.

[4] The abbreviations used are: AMPA, amino-3-hydroxy-5-methylisoxazole-4-propionic acid; AMPAR, AMPA receptor; NMDA, *N*-methyl-D-aspartic acid; NMDAR, NMDA receptor; KAR, kainate-type glutamate receptor; NTD, N-terminal domain; LBD, ligand-binding domain; TMD, transmembrane domain; TARP, transmembrane AMPA receptor regulatory protein; CUB, C1r/C1s-Uegf-BMP; LDLa, low-density lipoprotein class A; HA, hemagglutinin; PDB, Protein Data Bank; ANOVA, analysis of variance; IP, immunoprecipitation.

Beside the pore-forming subunits, native KARs and AMPARs associate with auxiliary proteins (13). Neto proteins bind KARs and regulate KAR deactivation, desensitization, rectification, and synaptic trafficking, similar to the effects of TARPs on AMPARs (14–16). Furthermore, Netos play critical roles in determining the axonal distribution of KARs in neurons (17, 18). Netos are also proposed to play a role in neural circuit development (19–21) and be required for normal fear expression (22, 23). Netos are single-pass transmembrane proteins with a long extracellular N-terminal sequence containing two Cir/C1s-Uegf-BMP (CUB) domains, a low-density lipoprotein class A (LDLa) domain, and a short intracellular C-terminal tail (24). Neto2 mutations in LDLa eliminate its effects on desensitization (25), and mutations in the intracellular C-terminal tail prevent the effects of Neto1/2 on rectification (26). Biochemical studies indicate that the CUB2 domain is critical for Neto protein binding to GluK2 (27). Nevertheless, the exact interaction between Netos and KARs remains elusive.

We previously reported that synaptic targeting of GluK1 in hippocampal CA1 neurons relies on Neto proteins, whereas that of GluK2 does not (11, 28). The differential trafficking properties and dependence on Netos between GluK1 and GluK2 rely on their NTDs (11, 29). We thus suspect that the NTDs of KARs might directly bind Neto proteins. Here we find that GluK2NTD specifically binds the CUB1 domain of Neto proteins. In addition, GluK2 without NTD (GluK2_core) can still bind to Neto proteins with or without the CUB1 domain. The effects of NTD-CUB1 and core-Neto interactions on GluK2 gating, including desensitization, deactivation, and recovery from desensitization, are systemically studied. Our data suggest a two-step model for Neto regulation of KAR gating and emphasize an important regulatory role for the NTD-CUB1 interaction.

Results

Netos interact with GluK2 through multiple sites

Previously, we found the synaptic targeting property of GluK1 and GluK2 is differentially regulated by Netos in an NTD-dependent manner (11, 28, 29), indicating that NTDs of KARs might directly interact with Netos. To test this hypothesis, we expressed the NTD of GluK2 by introducing a stop codon at position 401; thus, the NTD (residues 31–400) will be synthesized through the secretory ER pathway under the guidance of the signal peptide. To facilitate its detection, an HA tag was inserted after the signal peptide, and a FLAG epitope was inserted at the C termini of Netos. Consistent with our prediction, GluK2NTD was co-immunoprecipitated with Neto proteins (Fig. 1, *A* and *B*). We also observed that GluK2ΔNTD, in which the NTD was deleted, co-immunoprecipitated with Netos (Fig. 1, *A* and *B*), indicating that GluK2 interacts with Netos through multiple sites. In Netos, two CUB domains and an LDLa domain are located extracellularly. Which of these domains might interact with GluK2NTD? Because the NTD is the distal extracellular domain of KARs and is about 80 Å above the membrane plane (30), it is reasonable to suspect that the very distal CUB1 domain of Netos might interact with GluK2NTD. Indeed, GluK2NTD was efficiently co-immunoprecipitated with Neto1CUB1 or Neto2CUB1 (Fig. 1*C*). Meanwhile, GluK2ΔNTD was pulled down by Neto1/2ΔCUB1 (Fig. 1*D*), indicating a second interaction, which we named as the core-Neto interaction. Furthermore, deletion of CUB1 domains largely diminished Neto interaction with GluK2NTD (Fig. 1, *E–G*), suggesting that GluK2NTD specifically interacts with the CUB1 domains of Neto proteins. Thus, our observation suggested that GluK2 bind Netos through at least two interaction sites, the NTD-CUB1 interaction and the core-Neto interaction (Fig. 1*H*).

NTD truncation does not affect GluK2 desensitization and deactivation

Previous work demonstrated that NTD-truncated GluK2 receptors are functional (10). We thus used GluK2ΔNTD to study Neto related gating (Fig. S1*A*). Western blot analysis from cell lysate showed a similar expression level of GluK2ΔNTD and intact GluK2 receptors (Fig. S1*B*). Surface biotinylation revealed that the surface expression of GluK2 receptors was unaffected by NTD truncation (Fig. S1*B*). Furthermore, immunofluorescence experiments examining an HA tag inserted at N termini of full-length and NTD-deleted GluK2 showed that GluK2ΔNTD could express and traffic to the plasma membrane like full-length GluK2 receptors (Fig. S1*C*). Together, these observations suggest that the NTD is not required for GluK2 expression and membrane trafficking.

We then tested the effects of NTD truncation on gating kinetics by applying a saturating concentration of glutamate (10 mM) to outside-out patches excised from the transfected HEK cells using a fast piezoelectric system (25). The desensitization kinetics recorded by 500-ms application of glutamate displayed no difference between full-length and NTD-deleted GluK2 receptors (Fig. 2*A* and Fig. S2*A*). Similarly, the deactivation kinetics recorded by brief application (1 ms) of 10 mM glutamate was unchanged by NTD truncation (Fig. 3*A* and Fig. S2*B*). These observations are consistent with previous reports (10), suggesting that the NTD itself has little effect on the deactivation and desensitization kinetics of KARs.

NTD-CUB1 interactions distinguish Neto1 and Neto2 on desensitization

Previous work shows that Neto1 speeds and Neto2 slows GluK1 desensitization in a recombinant system or in neurons (28, 31). Similarly, Neto1 speeds and Neto2 slows GluK2 desensitization when overexpressed in hippocampal CA1 neurons (11). Here, we found in HEK cells that Neto2 dramatically slows the desensitization of GluK2 by ~4 times, whereas Neto1 has little effect (Fig. 2, *A* and *B*), indicating that Neto1 and Neto2 differentially regulate GluK2 desensitization. Interestingly, in the absence of NTD, GluK2ΔNTD was slightly slowed by both Neto1 and Neto2 (Fig. 2*C*) to a similar extent. When CUB1 domains of Netos were removed, GluK2 desensitization was not changed by Neto1ΔCUB1 or Neto2ΔCUB1 (Fig. 2*D*). Furthermore, GluK2ΔNTD desensitization was similarly slowed by Neto1ΔCUB1 and Neto2ΔCUB1 (Fig. 2*E*). These results thus demonstrated that the differential regulation of GluK2 desensitization by Neto1 and Neto2 relies on the NTD-CUB1 interaction. In addition, in the cases of ΔNTD (Fig. 2*C*), ΔCUB1

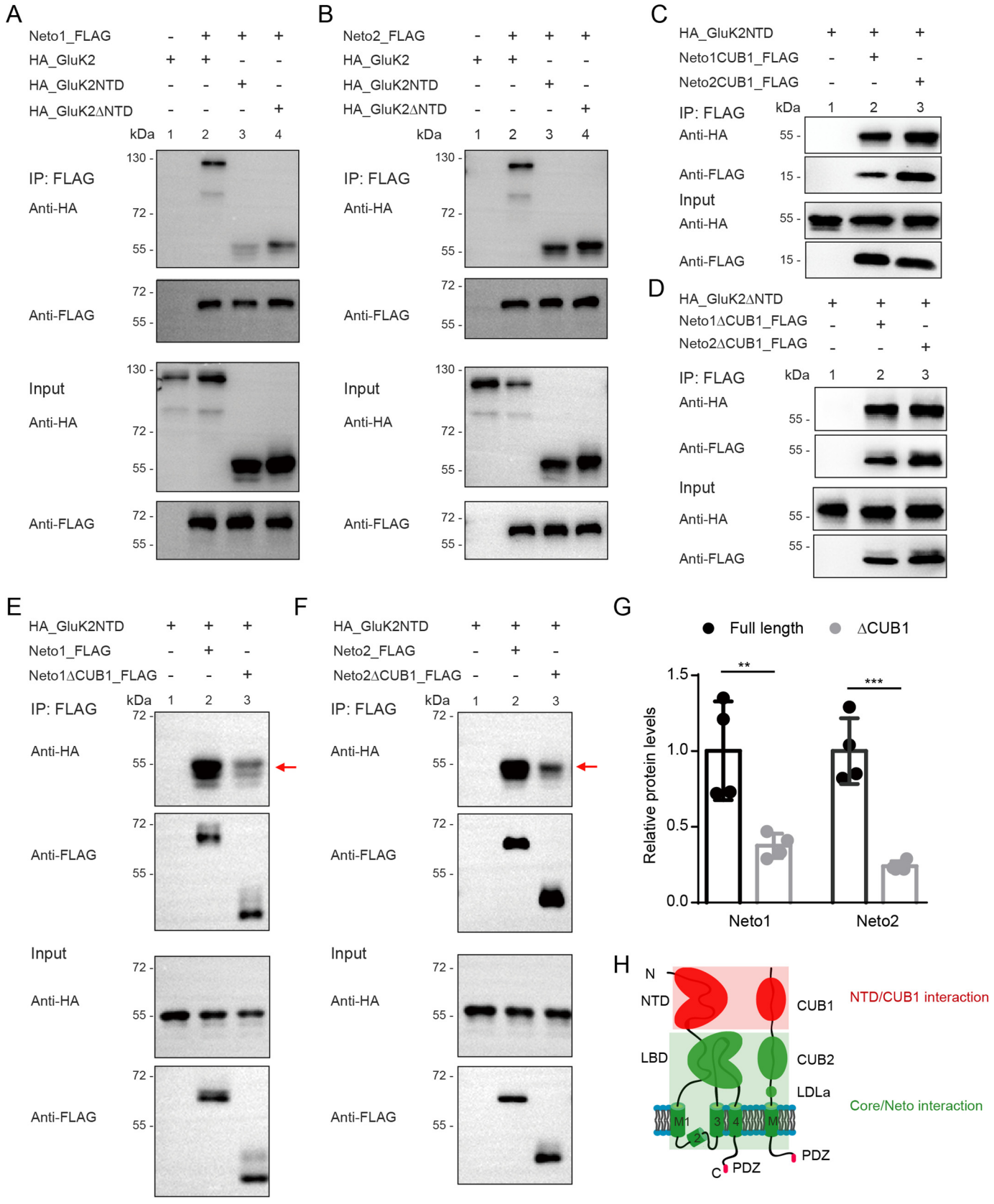
A
Neto1_FLAG - + + +
HA_GluK2 + + - -
HA_GluK2NTD - - + -
HA_GluK2ΔNTD - - - +
kDa 1 2 3 4
IP: FLAG
Anti-HA
Anti-FLAG
Input
Anti-HA
Anti-FLAG
130 -
72 -
55 -
B
Neto2_FLAG - + + +
HA_GluK2 + + - -
HA_GluK2NTD - - + -
HA_GluK2ΔNTD - - - +
kDa 1 2 3 4
IP: FLAG
Anti-HA
Anti-FLAG
Input
Anti-HA
Anti-FLAG
C
HA_GluK2NTD + + +
Neto1CUB1_FLAG - + -
Neto2CUB1_FLAG - - +
IP: FLAG
kDa 1 2 3
Anti-HA
Anti-FLAG
Input
Anti-HA
Anti-FLAG
55 -
15 -
D
HA_GluK2ΔNTD + + +
Neto1ΔCUB1_FLAG - + -
Neto2ΔCUB1_FLAG - - +
IP: FLAG
kDa 1 2 3
Anti-HA
Anti-FLAG
Input
Anti-HA
Anti-FLAG
55 -
E
HA_GluK2NTD + + +
Neto1_FLAG - + -
Neto1ΔCUB1_FLAG - - +
IP: FLAG
kDa 1 2 3
Anti-HA
Anti-FLAG
Input
Anti-HA
Anti-FLAG
72 -
55 -
F
HA_GluK2NTD + + +
Neto2_FLAG - + -
Neto2ΔCUB1_FLAG - - +
IP: FLAG
kDa 1 2 3
Anti-HA
Anti-FLAG
Input
Anti-HA
Anti-FLAG
72 -
55 -
G
Full length
ΔCUB1
Relative protein levels
1.5
1.0
0.5
0.0
**
***
Neto1
Neto2
H
N
NTD
CUB1
LBD
CUB2
LDLa
M1
3
4
M
2
C
PDZ
PDZ
NTD/CUB1 interaction
Core/Neto interaction

(Fig. 2*D*), and ΔNTD + ΔCUB1 (Fig. 2*E*), conditions in which NTD-CUB1 interactions were disrupted, KAR desensitization was generally slowed by Netos, indicating that the core-Neto interactions slow desensitization. Comparing the Neto effects on desensitization in Fig. 2*B* and those in Fig. 2 (*C–E*) leads to the conclusion that NTD-Neto1CUB1 speeds KAR desensitization and NTD-Neto2CUB1 slows it.

NTD-CUB1 interactions distinguish Neto1 and Neto2 on deactivation

We further studied the Neto regulatory effects on GluK2 deactivation. Neto2 but not Neto1 slowed GluK2 deactivation (Fig. 3*A* and Fig. S2*B*). Whereas the NTD was removed, GluK2ΔNTD was moderately slowed by Neto1 and Neto2 to a similar extent (Fig. 3*C*). When CUB1 domains were deleted, GluK2 deactivation was slightly slowed by Neto1ΔCUB1 and not by Neto2ΔCUB1 (Fig. 3*D*), but the effects of Neto1ΔCUB1 and Neto2ΔCUB1 were not significantly different. Furthermore, GluK2ΔNTD deactivation was slowed by Neto1ΔCUB1 and Neto2ΔCUB1 to similar extent (Fig. 3*E*). The results thus revealed that the different effects of Neto1 and Neto2 on GluK2 deactivation rely on the NTD-CUB1 interaction. Also, as with the desensitization data, it can be concluded that the core-Neto interactions slow deactivation in general. Taken together, these data revealed that the NTD-CUB1 interaction is critical for Neto1/2 modulation of GluK2 fast gating kinetics.

NTD deletion facilitates GluK2 recovery from desensitization

Deletion of NTDs of AMPA receptors facilitates their recovery from desensitization (7). We wondered whether this is the case for KARs. The recovery rate of full-length and NTD-deleted GluK2 receptors was monitored through a pair of glutamate (10 mM for 50 ms) applications with variable intervals. GluK2 receptors completely recovered from desensitization in seconds with a τ_{rec} value of 2.62 ± 0.54 s, similar to previous reports (25, 32). NTD truncation dramatically sped up this process by about 3 times (τ_{rec} = 0.91 ± 0.23 s) (Fig. 4 (*A* and *B*) and Fig. S3). These data thus suggest that the NTDs of KARs strongly inhibit the recovery from desensitization.

Netos speed the recovery rate of GluK2 but not GluK2ΔNTD

When GluK2 was coexpressed with Neto1 or Neto2, the recovery from desensitization were facilitated (Fig. 4*C*), consistent with previous reports (25, 31–33) that Netos speed KAR recovery. Thus, removal of NTD and coexpression with Netos had similar effects on GluK2 recovery from desensitization. Could these two manipulations have synergistic effects on the recovery rate? Very surprisingly, we found that the recovery rate of GluK2ΔNTD was notably slowed by Neto2 with τ_{rec} doubled but not by Neto1 (Fig. 4*D*). Neto2ΔCUB1 also slowed the recovery of GluK2 (Fig. 4*E*) and GluK2ΔNTD (Fig. 4*F*) by doubling the τ_{rec}, whereas Neto1ΔCUB1 had no effect (Fig. 4, *E* and *F*). Thus, data in Fig. 4 (*D–F*) indicate that core-Neto1 and core-Neto2 differentially regulate GluK2 recovery; core-Neto2 slows recovery, whereas core-Neto1 has no effect. Furthermore, the left shifting of the recovery curve by Netos in Fig. 4*C*, compared with the generally right shifting in the absence of NTD-CUB1 interaction (Fig. 4, *D–F*), indicated that NTD-CUB1 interaction speeds KAR recovery from desensitization.

The residues in Netos responsible for NTD-CUB1 interactions

Thus far, we have found that Neto proteins interact with GluK2 through at least two sites, the NTD and the core. NTD-CUB1 interaction plays an important role in regulating GluK2 gating. We thus wondered what exact sites are responsible for this interaction. We first made a model of the Neto2CUB1 domain by homology modeling using Deepview software. The spindle-shaped CUB1 domain was polarized according to its charge distribution (Fig. 5*A*). On one end of the molecule, positively charged arginine residues, including Arg^{50}, Arg^{81}, Arg^{83}, Arg^{131}, and Arg^{135}, are clustered to make the positive charge pole. On the other end, negatively charged Asp^{144}, Glu^{145}, Glu^{146}, and Glu^{148} composed the negative charge pole. We then examined whether these charges play a role in the interaction with GluK2NTD by mutating them to alanine residues. When the 4 negatively charged residues were mutated (DE4A), the Neto2CUB1 domain failed to pull down GluK2NTD (Fig. 5*B*, *arrow*), whereas mutation of the 5 positively charged residues (R5A) did not affect the pulldown efficiency. There are 3 negatively charged residues in the corresponding region in the Neto1CUB1 domain (Fig. 5*A*, *right*). Mutation of these negatively charged residues in the Neto1CUB1 domain (DE3A) also largely diminished the interaction with GluK2NTD (Fig. 5*C*, *arrow*). We further examined whether these negatively charged residues were responsible for the function of the NTD-CUB1 interaction. When the 4 negatively charged residues in Neto2 were mutated to alanines, the slowing of GluK2 desensitization by Neto2 was largely impaired (Figs. 2*B* and 5*D*). The Neto1(DE3A), in which the 3 negatively charged residues were mutated, slightly slowed GluK2 desensitization (Fig. 5*D*). Interestingly, when the negative charges neutralized, the regulatory effects on GluK2 desensitization were now the same between Neto1 and Neto2 (Fig. 5*D*), resembling the CUB1-deleted Netos (Fig. 2*D*). The mutated Netos failed to facilitate GluK2 recovery from desensitization, indicating that the NTD-CUB1 interaction was impaired (Fig. 5*E*), resembling CUB1 deletions (Fig. 4*E*).

Figure 1. Neto1/2 have two separate interaction sites with GluK2. *A* and *B*, immunoblotting of immunoprecipitates from transfected HEK293T cells. The identities of the transfected constructs were indicated *above* each *lane*. Full-length GluK2, GluK2NTD, and GluK2ΔNTD were co-immunoprecipitated with Neto1 and Neto2. *C*, GluK2NTD was co-immunoprecipitated with the CUB1 domains of Neto1/2. *D*, co-immunoprecipitation of GluK2ΔNTD and Neto proteins without CUB1 domains. *E* and *F*, co-immunoprecipitation of GluK2NTD and Neto proteins with or without CUB1 domains. Deletion of CUB1 domains significantly suppressed the interaction between GluK2 and Neto proteins (*arrows*). *G*, quantification of immunoprecipitation in *E* and *F*. The GluK2NTD pulled down was normalized by the FLAG signal pulled down. Compared with full-length Neto1 (1.00 ± 0.32), the GluK2NTD precipitated by Neto1ΔCUB1 was significantly reduced to 0.38 ± 0.08 (n = 4 pairs; **, $p < 0.01$, paired t test). Compared with full-length Neto2 (1.00 ± 0.22), the GluK2NTD pulled down by Neto2ΔCUB1 was significantly reduced to 0.24 ± 0.03 (n = 4 pairs; ***, $p < 0.001$, paired t test). *H*, a *schematic model* shows the two interaction sites between GluK2 and Neto proteins. *Error bars*, S.D.

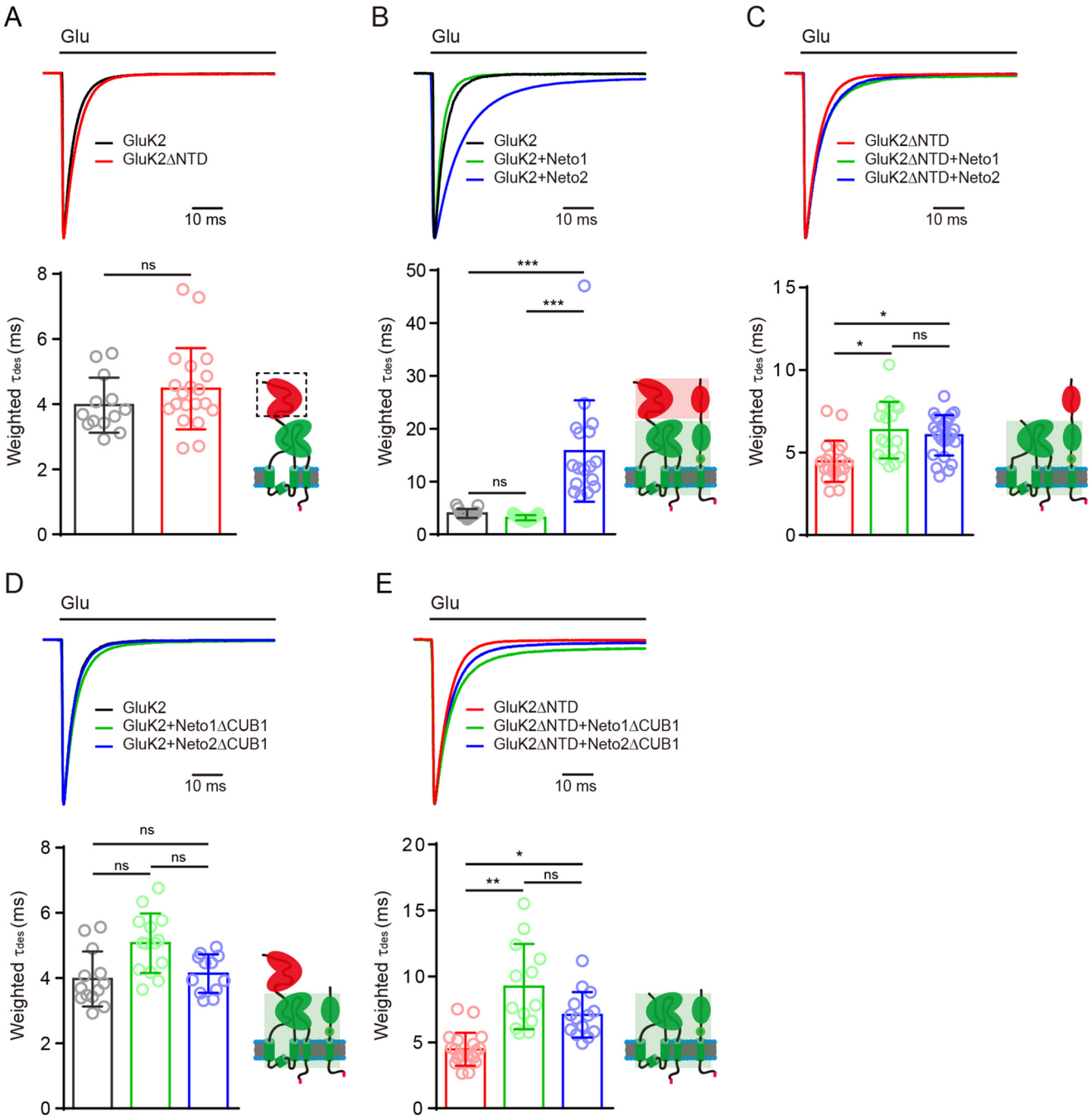

Figure 2. Neto regulation on GluK2 desensitization. *A*, deletion of NTD has no effect on GluK2 desensitization. *Top*, superimposed average desensitization traces of GluK2 and GluK2ΔNTD. *Bottom left*, statistical comparison between the τ_{des} of GluK2 and GluK2ΔNTD. *Bottom right*, a *schematic model* depicts deletion of NTD. *B*, modulatory effects of Neto1 and Neto2 on GluK2 desensitization. The *top panel* shows superimposed average desensitization traces. *Bottom left*, statistical comparison among the τ_{des} of GluK2 with and without Netos. Whereas Neto1 has no effect on GluK2 desensitization, Neto2 slows GluK2 desensitization by about 4 times (***, $p < 0.001$). Neto1 and Neto2 exhibited differential modulation on GluK2 desensitization (GluK2 + Neto1 *versus* GluK2 + Neto2; ***, $p < 0.001$). *Bottom right*, a *schematic model* depicts the NTD-CUB1 and core-Neto interactions. *C*, the modulatory effects of Neto1 and Neto2 on GluK2ΔNTD desensitization. The *top panel* shows superimposed average desensitization traces. *Bottom left*, statistical comparison among the τ_{des} of GluK2ΔNTD with and without Netos. Both Neto1 and Neto2 have modest slowing effects on GluK2ΔNTD (*, $p < 0.05$); no difference was found between GluK2ΔNTD + Neto1 and GluK2ΔNTD + Neto2. *Bottom right*, a *schematic model* depicts the core-Neto interaction under these conditions. *D*, CUB1-deleted Netos have no apparent effects on GluK2 desensitization. *E*, modulatory effects of CUB1-deleted Netos on GluK2ΔNTD. Neto1ΔCUB1 slowed the desensitization of GluK2ΔNTD (**, $p < 0.01$). Neot2ΔCUB1 slowed the desensitization of GluK2ΔNTD (*, $p < 0.05$). No significant difference was found between GluK2ΔNTD + Neto1ΔCUB1 and GluK2ΔNTD + Neto2ΔCUB1. The raw desensitization traces are depicted and the average desensitization traces are calculated in Fig. S2*A*. The data were analyzed using two-way ANOVA with post hoc Tukey's multiple-comparison tests (Netos or mutants, $F(4, 151) = 22.80$, $p < 0.001$; NTD, $F(1, 151) = 0.16$, $p = 0.69$; interaction, $F(4, 151) = 25.69$, $p < 0.001$). *, $p < 0.05$; **, $p < 0.01$; ***, $p < 0.001$; *ns*, not significant. *Error bars*, S.D.

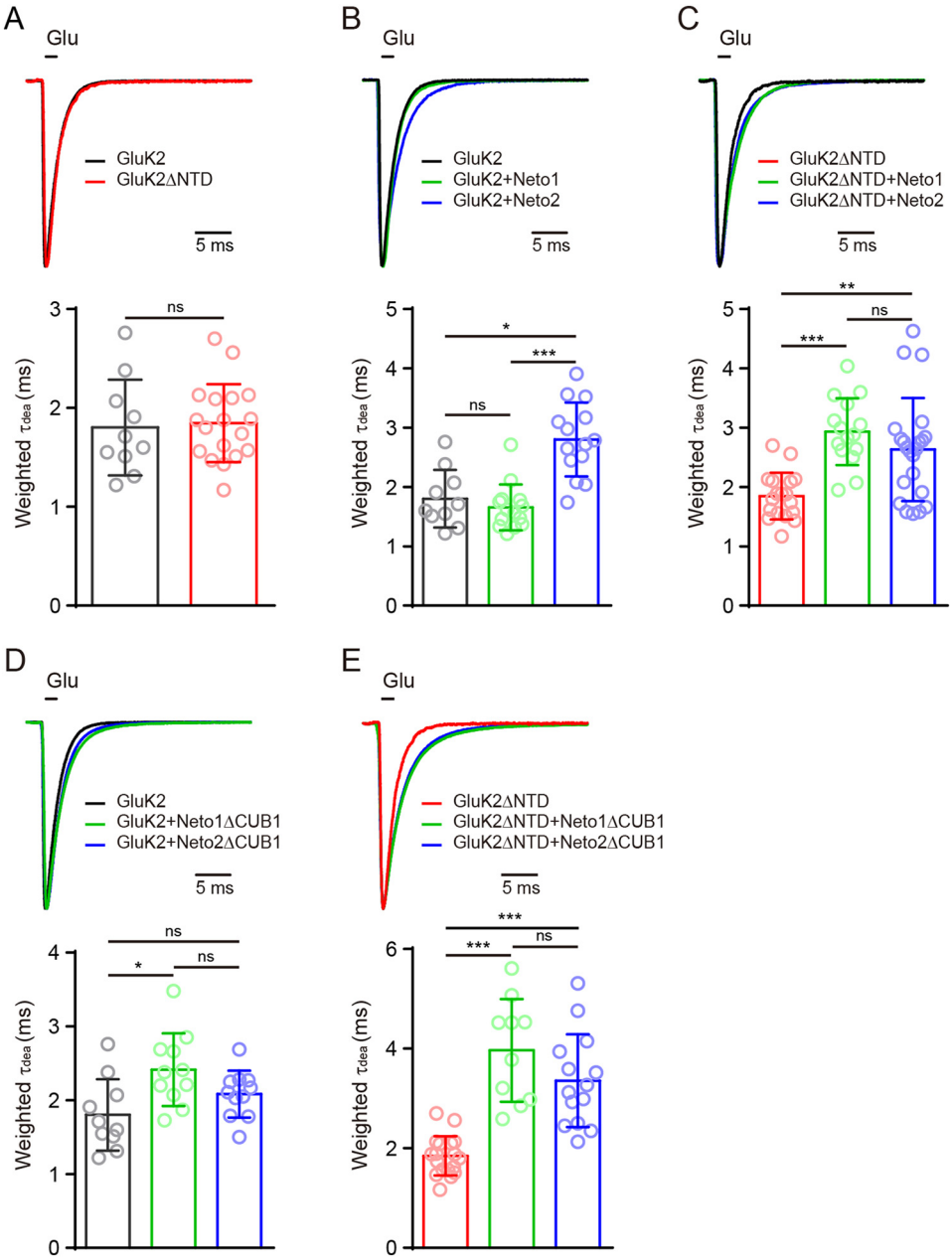

Figure 3. Neto regulation on GluK2 deactivation. *A*, deletion of NTD has no effect on GluK2 deactivation. *B*, modulatory effects of Neto1 and Neto2 on GluK2 deactivation. *Top*, superimposed average deactivation traces. *Bottom*, whereas Neto1 has no effect on GluK2 desensitization, Neto2 slows GluK2 deactivation (*, $p < 0.05$). Neto1 and Neto2 exhibited differential modulation on GluK2 deactivation (GluK2 + Neto1 *versus* GluK2 + Neto2; ***, $p < 0.001$). *C*, modulatory effects of Neto1 and Neto2 on GluK2ΔNTD deactivation. *Top*, superimposed average desensitization traces. *Bottom*, both Neto1 and Neto2 have modest slowing effects on GluK2ΔNTD (*, $p < 0.05$). No difference was found between GluK2ΔNTD + Neto1 and GluK2ΔNTD + Neto2. *D*, Neto1ΔCUB1 slightly slowed (*, $p < 0.05$), whereas Neto2ΔCUB1 has no effect on GluK2 deactivation. However, the effects were not significantly different between Neto1ΔCUB1 and Neto2ΔCUB1. *E*, modulatory effects of CUB1-deleted Netos on GluK2ΔNTD deactivation. Both Neto1ΔCUB1 and Neto2ΔCUB1 slowed the deactivation of GluK2ΔNTD (***, $p < 0.001$). No significant difference was found between GluK2ΔNTD + Neto1ΔCUB1 and GluK2ΔNTD + Neto2ΔCUB1. The raw deactivation traces are depicted and the average deactivation traces are calculated in Fig. S2*B*. The data were analyzed using two-way ANOVA with post hoc Tukey's multiple-comparison tests (Netos or mutants, $F(4, 129) = 14.68$, $p < 0.001$; NTD, $F(1, 129) = 47.39$, $p < 0.001$; interaction, $F(4, 129) = 10.00$, $p < 0.001$). *, $p < 0.05$; **, $p < 0.01$; ***, $p < 0.001$; *ns*, not significant. *Error bars*, S.D.

The residues in GluK2NTD responsible for NTD-CUB1 interactions

Because the negatively charged pole on the CUB1 domains is responsible for the interaction with GluK2NTD, we suspect that a positively charged patch on the GluK2NTD surface might interact with CUB1s. We then searched the surface of GluK2NTD for highly positively charged regions. The GluK2NTD dimer was adapted from the full-length GluK2 cryo-EM structure (PDB entry 5KUF). We identified six positively charged clusters that contain at least 2 positively charged residues (shown in *blue* in Fig. 6*A*) from one subunit of the NTD dimer. The positively charged regions were neutralized by mutating lysine and arginine residues to alanine residues (Fig. 6*A*). Other positively charged residues scattered on the NTD surface were not touched (shown in *pink* in Fig. 6*A*). Pulldown experiments showed that when group 1 positively charged

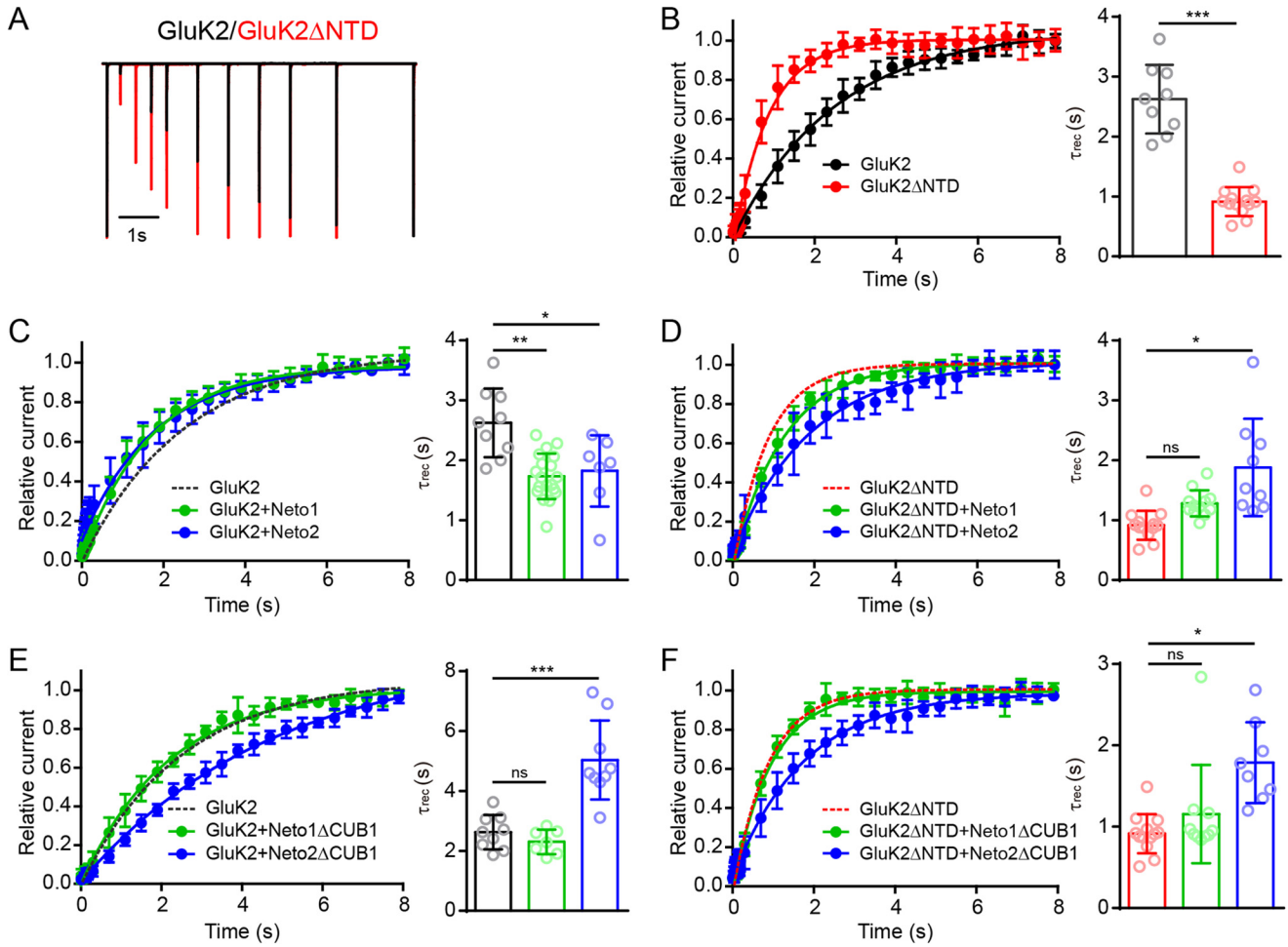

Figure 4. Neto regulation on GluK2 recovery from desensitization. *A*, representative recording traces of GluK2 and GluK2ΔNTD evoked by pairs of 50-ms applications of 10 mM glutamate. The interval time between two applications ranged from 5 to 8000 ms. The amplitude was normalized to the first peak. *B*, analysis of the recovery rates of GluK2 and GluK2ΔNTD. *Left*, the recovery was calculated by the peak amplitude of the second response divided by that of the first response. Data points represent mean ± S.D. The average data were fitted with a single-exponential equation (*black*, GluK2; *red*, GluK2ΔNTD). *Right*, the time constants (τ_{rec}) were compared between GluK2 and GluK2ΔNTD. Deletion of NTD significantly sped the receptor recovery from desensitization (***, $p < 0.001$). *C*, Netos regulate GluK2 recovery from desensitization. Both Neto1 and Neto2 sped GluK2 recovery from desensitization ($p < 0.05$ (*) and $p < 0.01$ (**), respectively). *D*, Netos differentially regulate GluK2ΔNTD recovery from desensitization. Neto1 has no effect on GluK2ΔNTD recovery from desensitization. Neto2 slowed GluK2ΔNTD recovery from desensitization (*, $p < 0.05$). *E*, CUB1-deleted Netos differentially regulate GluK2 recovery from desensitization. Neto1ΔCUB1 has no effect on GluK2 recovery from desensitization. Neto2ΔCUB1 slowed GluK2 recovery from desensitization (***, $p < 0.001$). *F*, CUB1-deleted Netos differentially regulate GluK2ΔNTD recovery from desensitization. Neto1ΔCUB1 has no effect on GluK2ΔNTD recovery from desensitization. Neto2ΔCUB1 slowed GluK2ΔNTD recovery from desensitization (*, $p < 0.05$). The representative traces for recovery from desensitization are depicted in Fig. S3. The data were analyzed using two-way ANOVA with post hoc Tukey's multiple-comparison tests (Netos or mutants, $F(4, 93) = 29.92$, $p < 0.001$; NTD, $F(1, 93) = 109.80$, $p < 0.001$; interaction, $F(4, 93) = 20.22$, $p < 0.001$). *, $p < 0.05$; **, $p < 0.01$; ***, $p < 0.001$; *ns*, not significant. *Error bars*, S.D.

residues in GluK2NTD were mutated, the interaction with Neto2CUB1 was largely diminished, whereas mutations on groups 2–6 did not affect NTD interaction with Neto2CUB1 (Fig. 6*B*). The group 1 residues contain Arg^{50}, Lys^{82}, Lys^{93}, and Lys^{94}. Neither single mutation of these residues nor double mutations of Arg^{50} and Lys^{82} affected the pulldown efficiency (Fig. 6*C*). These data suggest that the positively charged residues in group 1 are redundant. We then examined the functional effects of mutating these positively charged residues. GluK2(RK4A), in which 4 positively charged residues (Arg^{58}, Lys^{82}, Lys^{93}, and Lys^{94}) were mutated to alanines, was modestly slowed by Neto1 and Neto2 (Fig. 6*D*), resembling the effect of NTD deletion (Fig. 2*D*). Netos failed to facilitate the recovery of GluK2(RK4A) from desensitization (Fig. 6*E*), indicating that the NTD-CUB1 interaction was impaired with these mutations, resembling that of GluK2ΔNTD (Fig. 4*D*).

Differential regulation of desensitization does not simply rely on CUB1s

Neto1 and Neto2 have significant differential effects on GluK2 fast gating, especially on the desensitization kinetics. Our deletion and mutation experiments indicate that the CUB1 domains might account for the difference. To test this hypothesis, we made chimeric constructs of Netos by swapping the CUB1 domains (Fig. S4*A*). Indeed, Neto1(Neto2CUB1), Neto1 harboring Neto2CUB1, slowed GluK2 desensitization compared with Neto1, but the slowing effect was much less than that of Neto2 (Fig. S4, *B* and *C*). On the other hand, Neto2(Neto1CUB1) slowed GluK2 desensitization just like Neto2 (Fig. S4, *B* and *C*). These data thus indicate that the difference in CUB1 sequences, at most, only partially accounts for the differential regulatory effects on GluK2 fast gating by Netos.

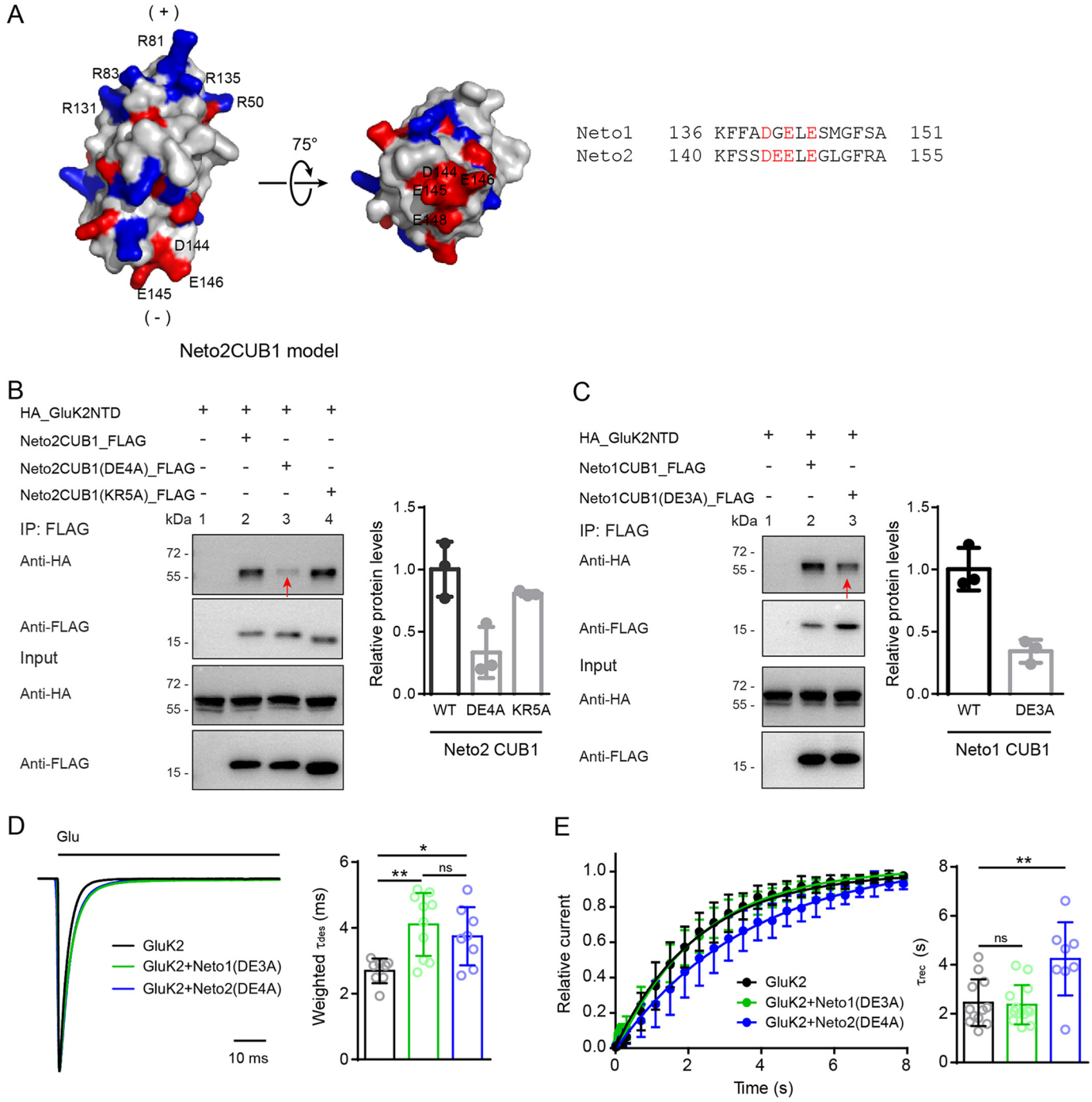

Figure 5. Critical residues on CUB1 domains for NTD-CUB1 interactions. *A*, homology model for Neto2CUB1 domain. *Left*, distribution of the charges on the Neto2CUB1 surface. Negatively charged residues are shown in *red*, and positively charged residues are shown in *blue*. The molecule is polarized according to its charge distribution. *Middle*, the model is rotated for better view of the negatively charged pole. *Right*, sequence alignment around the negatively charged residues between Neto1 and Neto2. *B*, co-immunoprecipitation of Neto2CUB1 mutants with GluK2NTD. The interaction between GluK2NTD and Neto2CUB1 was significantly diminished when 4 negatively charged residues were mutated to alanine residues (*arrow*). The mutation of 5 residues on the positively charged pole did not affect CUB1 interaction with GluK2NTD. *Right*, bar graph shows the relative pulldown efficiency from three experiments. The GluK2NTD pulled down was normalized by the FLAG signal pulled down. *C*, mutation of the 3 negatively charged residues in Neto1CUB1 domain diminished its binding to GluK2NTD (*arrow*). *Right*, bar graph shows the relative pulldown efficiency from three experiments. The GluK2NTD pulled down was normalized by the FLAG signal pulled down. *D*, neutralization of the negative charges affects Neto regulation on GluK2 desensitization. *Left*, superimposed average desensitization traces of GluK2 with or without mutated Netos recorded in a parallel experiment. *Right*, *bar graph* shows the weighted τ_{des}. GluK2, 2.69 ± 0.35 ms, $n = 8$; GluK2 + Neto1(DE3A), 4.10 ± 0.91 ms, $n = 10$; GluK2 + Neto2(DE4A), 3.75 ± 0.83 ms, $n = 8$. One-way ANOVA with post hoc Tukey's multiple comparisons tests was used: $F(2, 23) = 7.24$, $p < 0.01$. *, $p < 0.05$; **, $p < 0.01$; *ns*, not significant. *E*, neutralization of the negative charges affects Neto regulation on GluK2 recovery from desensitization. *Left*, recovery of GluK2 with or without mutant Netos recorded in a parallel experiment. *Right*, analysis of the recovery rates. GluK2 + Neto1(DE3A) (2.36 ± 0.77 s, $n = 13$) was not different from GluK2 (2.45 ± 0.92 s, $n = 12$). Neto2(DE4A) slowed GluK2 recovery (4.24 ± 1.40 s, $n = 8$; **, $p < 0.01$, one-way ANOVA with post hoc Tukey's multiple comparisons, $F(2, 30) = 9.17$, $p < 0.001$). *Error bars*, S.D.

NTD-CUB1 interactions do not affect rectification

Another biophysical property of KARs affected by Netos is voltage-dependent blockage by polyamines (26, 34). We examined the rectification property of GluK2 receptors after NTD truncation in the presence of concanavalin A to prevent desensitization (35). NTD deletion enhanced rectification (Fig. S5, *A* and *B*), reducing the rectification index (Fig. S5*C*). Both Neto1 and Neto2 markedly reduced the inward rectification of full-length GluK2 receptor (Fig. S5, *A* and *C*) and GluK2ΔNTD (Fig. S5, *B* and *C*). Neto1 effects were relatively stronger than those of

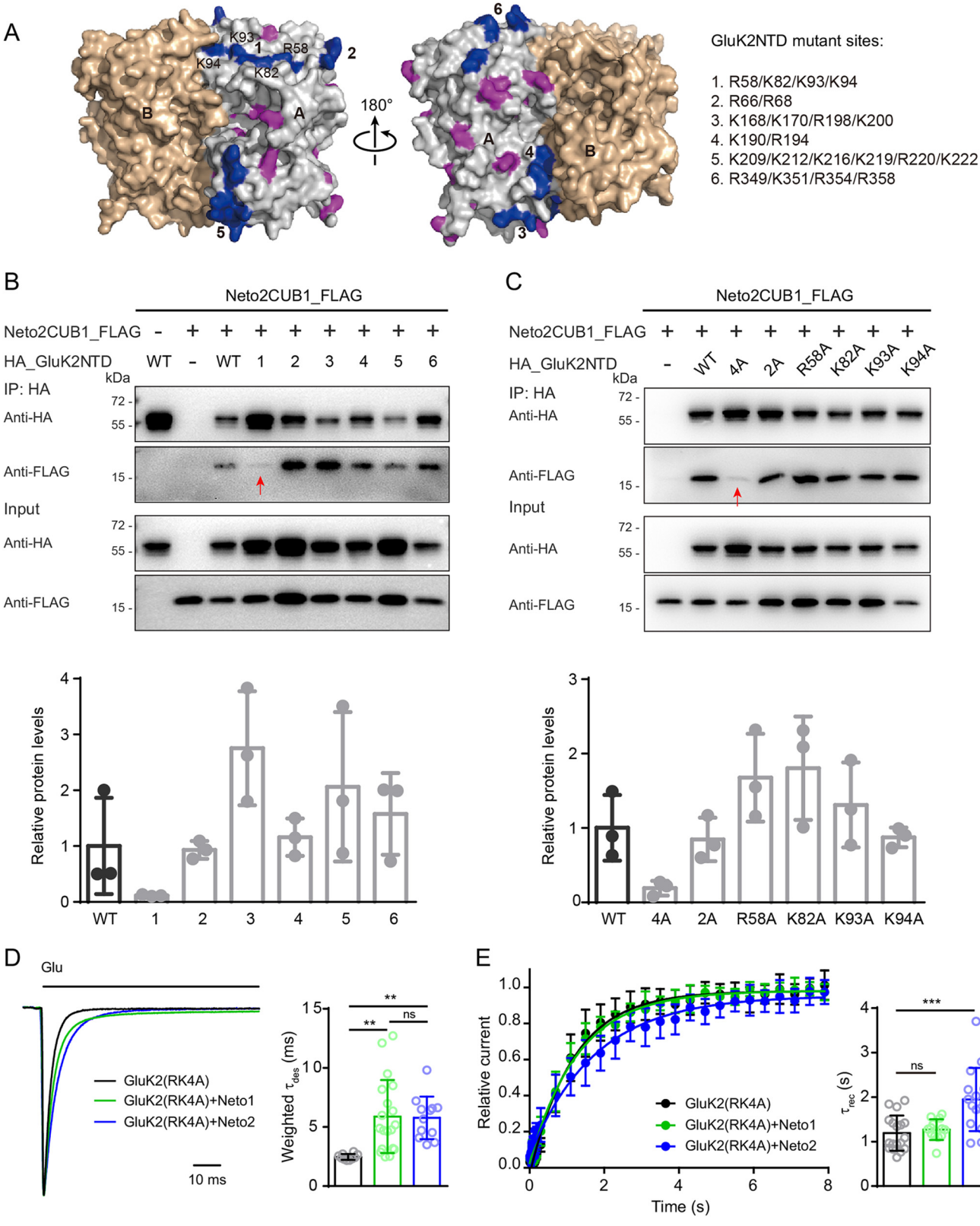

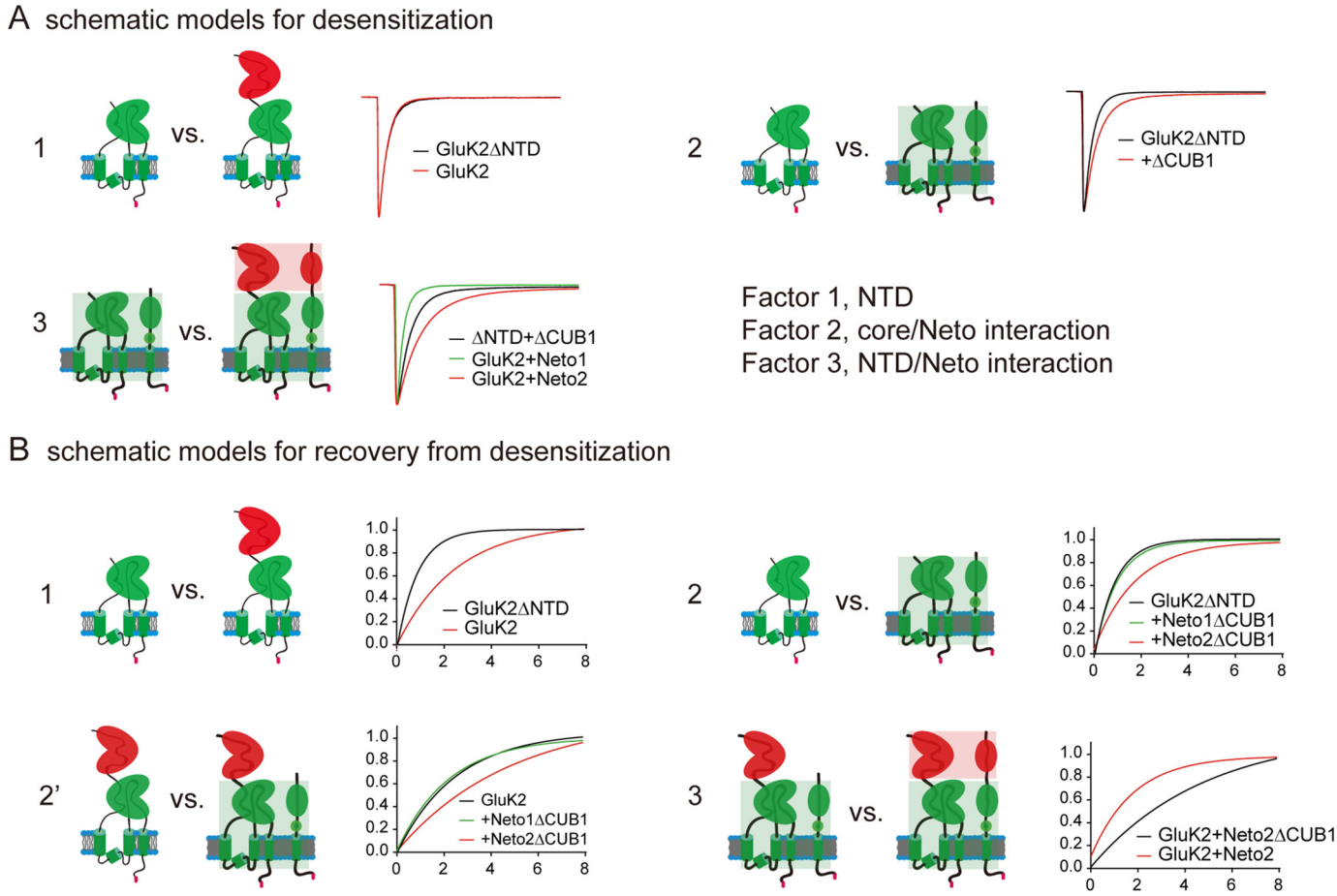

Figure 7. *Schematic models* summarizing NTD and Neto modulation of GluK2 gating. *A*, effects of the three factors, NTD, core-Neto interaction, and NTD-CUB1 interaction, on GluK2 desensitization. The model starts from the smallest functional receptor, GluK2ΔNTD. NTD has no effect on desensitization (*comparison 1*). Core-Neto interaction with either Neto1 or Neto2 slows desensitization (*comparison 2*). NTD-Neto1 speeds up desensitization, whereas NTD-Neto2 slows desensitization (*comparison 3*). These models can be applied for GluK2 deactivation. *B*, the three factors on the recovery from desensitization. Among the three factors, NTD appears to have most dramatic effects and stabilizes the receptor in the desensitization state (*comparison 1*). Core-Neto1 has little effect, whereas core-Neto2 slows the recovery speed either on NTD-truncated (*comparison 2*) or full-length GluK2 (*comparison 2'*). The NTD-CUB1 interaction speeds GluK2 recovery (*comparison 3*).

Neto2. These data thus suggested the GluK2 NTD is not involved in Neto modulation of receptor rectification.

Discussion

In the present study, we have experimentally defined two interactions between GluK2 receptor and auxiliary Neto proteins. The GluK2NTD directly interacts with Neto proteins through binding to CUB1 domains, defining the NTD-CUB1 interactions. The core of GluK2 interacts with Neto domains other than CUB1, defining a second core-Neto interaction. The NTD-CUB1 interaction involves the static electric attraction between a negatively charged cluster in CUB1 domains and a positively charged patch on the surface of GluK2NTD.

By coexpression of NTD-truncated GluK2 and CUB1-truncated Netos, we have systemically examined 1) the NTD alone, 2) the core-Neto interaction, and 3) the NTD-CUB1 interaction on KAR gating, including desensitization, deactivation, and recovery from desensitization. The three factors have different effects on GluK2 fast gating (deactivation and desensitization) and slow gating (recovery from desensitization). To facilitate the understanding of our data, we made schematic models (Fig. 7) and started from the smallest functional receptor,

Figure 6. Critical residues in GluK2NTD for NTD-CUB1 interaction. *A*, the NTD dimer of GluK2 is adapted from the cryo-EM structure of GluK2 (PDB entry 5KUF). Highly positive patches on the surface of subunit A containing at least two positively charged residues were identified (in *blue*). Positively charged residues scattered on the NTD surface are shown in *pink*. *Right*, residues composed of the six highly positive patches on the NTD surface. *B*, co-immunoprecipitation of Neto2CUB1 domain coexpressed with GluK2NTD with or without mutations. *Lanes 1–6*, GluK2NTD mutations carrying alanine replacement of positively charged residues identified in *A*. The interaction between GluK2NTD and the CUB1 domain was significantly disrupted when the 4 positively charged residues in group 1 were mutated to alanine residues (*arrow*). *Bottom*, the *bar graph* shows the pulldown efficiency from three experiments. *C*, co-immunoprecipitation of Neto2CUB1 domain with GluK2NTD mutations. *4A*, the same mutant as *lane 1* in *B*. *2A*, R58A_K82A. The interaction between GluK2NTD and CUB1 domain was significantly disrupted in the 4A mutation of the GluK2NTD but not in single or double mutations. *Bottom*, the *bar graph* quantifies the pulldown efficiency from three experiments. *D*, Neto1 and Neto2 regulation on the desensitization of GluK2(RK4A). Both Neto1 (5.89 ± 3.01 ms, $n = 19$) and Neto2 (5.78 ± 1.72, $n = 12$) slowed the desensitization of GluK2(RK4A) (2.47 ± 0.23 ms, $n = 10$). **, $p < 0.01$, one-way ANOVA with post hoc Tukey's multiple comparisons, $F(2, 30) = 9.17$, $p < 0.001$. *E*, GluK2(RK4A) recovery from desensitization with or without Netos. Neto1 (1.27 ± 0.22 s, $n = 13$) had no effect on GluK2(RK4A) recovery (1.19 ± 0.38 s, $n = 18$). Neto2 (1.95 ± 0.69 s, $n = 15$) slowed GluK2(RK4A) recovery. ***, $p < 0.001$; *ns*, not significant, one-way ANOVA with post hoc Tukey's multiple comparisons, $F(2, 43) = 11.08$, $p < 0.001$. *Error bars*, S.D.

GluK2ΔNTD. For fast gating, such as desensitization, comparison 1 in Fig. 7*A* suggests that NTD alone has no effect on GluK2 desensitization. Comparison 2 in Fig. 7*A* suggests that core-Neto interactions slow KAR desensitization. Comparison 3 in Fig. 7*A* suggests that NTD-Neto1CUB1 interaction speeds desensitization whereas NTD-Neto2CUB1 slows desensitization. For recovery from desensitization, comparison 1 in Fig. 7*B* suggests that NTD has strong inhibitory effects on GluK2 recovery. Comparison 2 and 2′ in Fig. 7*B* suggest that core-Neto1 has no effect on KAR recovery from desensitization, whereas core-Neto2 slows the recovery. Comparison 3 in Fig. 7*B* suggests that NTD-CUB1 interactions facilitate GluK2 recovery.

Following the discovery of Netos as KAR auxiliary subunits, numerous studies have explored Neto regulation on KAR kinetics, mostly through recombinant systems or through overexpression in neurons. A general conclusion is that the Neto regulation of KARs is receptor subunit–specific and Neto isoform–specific. Neto1 speeds GluK1 desensitization in recombinant systems as well as overexpression in hippocampal CA1 neurons (28, 31). Neto1 speeds GluK2 desensitization in hippocampal CA1 neurons (11) but not in HEK cells (this study). Neto1 has relatively little or no effect on GluK1 or GluK2 deactivation in neurons (11, 28). In contrast, Neto2 significantly slows the desensitization and deactivation of GluK1 and GluK2 in either recombinant systems or neurons (11, 25, 28, 36). We find that deleting the NTD has no effect on GluK2 decay kinetics. Interestingly, the core-Neto interactions by Neto1 and Neto2 similarly slow the desensitization and deactivation of GluK2 under five conditions when NTD-CUB1 interactions are disrupted: deletion of the NTD, deletion of the CUB1, deletion of both, mutation of the CUB1 negative charges, or mutation of GluK2NTD positive charges (Figs. 2 (*C–E*), 3 (*C–E*), 5*D*, and 6*D*). Only when full-length WT Neto1/2 are co-expressed with GluK2 are the desensitization and deactivation dramatically different between Neto1 and Neto2 (Figs. 2*B* and 3*B*). Therefore, the differential modulatory effects of Neto1 and Neto2 on GluK2 desensitization and deactivation rely on the CUB1 interaction with the NTD of KARs. However, the sequence difference in CUB1 domains cannot explain the differential regulatory effects of Neto1 and Neto2 on GluK2 fast gating kinetics. By switching the CUB1 domains, the desensitization kinetics are not switched (Fig. S4). Fisher (32) found that switching both the CUB1 and CUB2 domain between Neto1/2 can largely (yet incompletely) switch the differential gating properties on GluK1. Therefore, the Neto isoform–specific modulation on KAR fast gating might require a more sophisticated stereoscopic interaction between NTD and CUB1. In addition, a more complicated allosteric modulation between NTD-CUB1 and core-Neto interactions might exist. To fully understand the differential modulatory effects by Neto1 and Neto2 will require a structural picture of the GluK/Neto complex in the future.

One interesting property of the NTDs of glutamate receptors is their effect on the recovery from desensitization. NMDARs have little desensitization, whereas non-NMDARs, AMPARs and KARs, desensitize soon after activation and recover in variable time intervals (37). GluK2 fully recovers from desensitization in seconds, whereas AMPARs recover in hundreds of milliseconds (25, 38, 39). During desensitization, the association of LBD dimers ruptures and rearranges into quasi-4-fold architecture (6, 37, 40). Additionally, NTD dimers of GluA2 receptors appear to separate, whereas the NTD dimers of GluK2 receptors remain undisrupted. This may explain why GluK2 is much more stable in the desensitized state compared with GluA2 receptors (40–42). NTD-truncated GluK2 receptors desensitize at the same rate as intact receptors (Fig. 2*A*) but recover 3 times faster (Fig. 4*B*). These results are consistent with the structural observations suggesting that NTDs stabilize the desensitized state of AMPARs (7) or KARs.

Netos were reported to facilitate the recovery from desensitization of variable homomeric and heteromeric KARs (14, 25, 31–33, 36). We also observed the facilitation of GluK2 recovery by Netos, which completely rely on the NTD-CUB1 interactions. Under all conditions where NTD-CUB1 interactions are disrupted, including deletion of the NTD and/or CUB1, and mutations on the interface, the core-Neto interactions generally stabilize the desensitized states and slow the recovery. For this effect, Neto2 is much stronger than Neto1.

A large number of studies suggest that KARs interact with Netos at multiple sites. From the Neto side, CUB domains, LDLa, TMD, and C-terminal domain are involved (25, 26, 32). However, which domains of KARs are involved in the interaction remains largely unclear. A previous study suggested that the linker between M3 and S2 is important for Neto-related gating (43). Our biochemical results demonstrate that both the isolated NTD and the GluK2ΔNTD are able to bind Netos, consistent with the notion that KARs bind Netos through multiple sites. Functionally, the NTD-CUB1 interactions and core-Neto interactions have differential effects on GluK2 deactivation, desensitization, and recovery from desensitization, suggesting a two-step model for Neto regulation of KAR gating (Fig. 7).

Materials and methods

Molecular biology

GluK2 (Q form) and Neto2 from rats and Neto1 from mice were used in this study. To ensure the co-expression of Neto proteins and GluK2 receptor in the same HEK293T cells, the cDNA of GluK2 was subcloned into vector pCAGGS-IRES-EGFP, whereas Neto1 and Neto2 were subcloned into vector pCAGGS-IRES-mCherry (28). Mutations in GluK2 and Netos were made by overlapping PCR. Specifically, GluK2ΔNTD was made by deletion of Thr^{32}–His^{400} of GluK2 without disruption of the signal peptide (residues 1–31). Additionally, we subcloned the NTD together with the signal peptide into vector pCAGGS-IRES-EGFP to construct isolated NTD. For pulldown experiments, an HA tag was inserted into GluK2 constructs after the sequence of signal peptide, and a FLAG tag was inserted into C termini of Neto1 and Neto2 constructs. All of the constructs were confirmed using sequencing over the entire length of the coding region.

Western blotting

HEK293T cells were cultured using Dulbecco's modified Eagle's medium with 10% fetal bovine serum, and passaged

every 2 days. In the Western blotting experiment, HEK293T cell were transiently transfected using Lipofectamine 2000 reagent (Invitrogen) following the manufacturer's instructions. The vectors used in transfection were GluK2 (mutation)/Neto (mutation) = 1:1 for biochemical experiments. 4 h later, medium was changed, and 100 μM DNQX (Abcam) was added to block GluK2 receptor currents. Cells were lysed in radioimmune precipitation assay buffer 48 h later. The cell lysates were kept on the ice for 30 min and then centrifuged at 13,800 $\times$ *g* at 4 °C for 30 min. After centrifugation, the supernatant was transferred to a new tube and completely mixed with 4$\times$ loading buffer. Then the mix was immediately loaded into 8% SDS-polyacrylamide gels in the presence of DTT. The protein bands were transferred to polyvinylidene difluoride membranes (Millipore) at 100 V for 2 h and then blocked in 5% nonfat milk dissolved in TBST at room temperature for 1 h. Finally, the level of GluK2 receptor and Neto proteins were probed with anti-HA antibody (Sigma, H3663), anti-FLAG antibody (Sigma, F3165), or anti-C-terminal GluR6/7 (Merck Millipore, 04-921), respectively, and detected using the ECL substrate (Thermo) before exposure.

Cell surface biotinylation

Cells were washed three times with ice-cold PBS before 1 mM solution of Sulfo-NHS-LC-Biotin (Thermo Fisher Scientific, catalogue no. 21335) in PBS for biotinylating cell surface proteins. After incubating at 4 °C for 30 min, reactions were quenched with 50 mM glycine, followed by rinsing three times with ice-cold TBS. Cells were then scraped in radioimmune precipitation assay buffer (50 mM Tris-HCl, 150 mM NaCl, 1% Triton X-100, 1% sodium deoxycholate, 0.1% SDS, 10 mM sodium phosphate, 2 mM EDTA, and 0.2% sodium vanadate) supplemented with a mixture of protease inhibitors (Roche Applied Science) and solubilized for 1 h at 4 °C. Nonsolubilized particles were removed by centrifugation at 13,800 $\times$ *g* for 10 min at 4 °C. The solubilized protein concentration was determined by BCA assay and mixed with monomeric avidin-agarose beads (Thermo Fisher Scientific, catalogue no. 20228). The mixture was incubated for 1 h with rotation at room temperature. Beads were subsequently washed three times with PBS. Finally, proteins were eluted by boiling in Laemmli buffer and then separated by electrophoresis on 8% SDS-polyacrylamide gels.

Immunocytochemistry and confocal microscopy

Cell surface receptors were detected by nonpermeabilized immunocytochemistry. HEK293T cells were washed in PBS and fixed in 4% paraformaldehyde in PBS. After blocking in normal goat serum, cell surface GluK2 or GluK2ΔNTD staining was examined using mouse anti-HA antibody (Sigma, H3663), followed by goat anti-mouse Alexa 549 secondary antibody. Samples were then permeabilized with 0.1% Triton X-100, and total GluK2 content was determined by staining with rabbit anti-C-terminal GluR6/7 (Merk Millipore, 04-921) and goat anti-rabbit Alexa 488. After the secondary antibody was washed by PBS three times, the cells were additionally incubated with Hoechst 33258 for nuclear staining. Samples were examined and analyzed through a $\times$63 oil immersion lens on a Zeiss LSM880 microscope.

Immunoprecipitation

Transfected cells were washed three times with PBS and harvested and solubilized in lysis buffer (50 mM Tris-Cl, pH 7.2, 150 mM NaCl, 2 mM EDTA, and 0.1% Triton X-100), supplemented with a mixture of protease inhibitors (Roche Applied Science) and solubilized for 1 h at 4 °C. After centrifugation at 13,800 $\times$ *g* for 10 min, the pellet was discarded. Lysates were then incubated with antibodies at 4 °C overnight. Then lysates were incubated with Protein G beads (GE Healthcare) for 2 h at 4 °C on a rotating platform. After incubation, beads were washed four times with lysis buffer and boiled in 40 μl of 2$\times$ Laemmli buffer. The mixtures were then centrifuged at 13,800 $\times$ *g*, and the supernatant was used for detection by Western blotting. For all samples, 1% of that used for IPs was used for input in gel analysis.

Electrophysiology

Whole-cell electrophysiology recording—Whole-cell recording was performed on transfected HEK293T cells as described previously (44). The vectors used in transfection for electrophysiology recording were GluK2 (mutation)/Neto (mutation) = 1:2 to ensure that Netos were expressed in sufficient amounts compared with GluK2. The cells were bathed in the extracellular solution: 145 mM NaCl, 2.5 mM KCl, 1 mM $CaCl_2$, 1 mM $MgCl_2$, 10 mM glucose, and 10 mM HEPES (pH 7.4). The positively transfected cells were identified by fluorescence via epifluorescence microscopy. Whole-cell patches were performed with glass pipettes (3–5 megaohms) filled with intracellular solution: 140 mM CsCl, 4 mM $MgCl_2$, 1 mM EGTA, 10 mM HEPES, 4 mM Na_2ATP, 0.1 mM spermine (pH 7.4). Before recording, the transfected cells were incubated with 1 mg/ml concanavalin A for at least 5 min to prevent GluK2 receptor desensitization. The current-voltage curves were recorded with a ramp voltage protocol from −100 to +100 mV in a period of 700 ms 10 times in the presence of 1 mM glutamate diluted in extracellular solution. All of the currents were collected with an Axoclamp 700B amplifier and Digidata 1440A (Molecular Devices, Sunnyvale, CA), filtered at 3 kHz, and digitized at 10 kHz. The current data were analyzed using Clampfit software.

Outside-out patch recording—The outside-out patches was pulled from transfected HEK293T cells and recorded as reported previously (25). The external solution was 140 mM NaCl, 2.5 mM KCl, 2 mM $CaCl_2$, 1 mM $MgCl_2$, 5 mM glucose, and 10 mM HEPES (pH 7.4). Patch pipettes (resistance 3–5 megaohms) were filled with a solution containing 130 mM KF, 33 mM KOH, 2 mM $MgCl_2$, 1 mM $CaCl_2$, 11 mM EGTA, and 10 mM HEPES (pH 7.4). 10 mM glutamate diluted into the external solution was applied with θ glass pipettes mounted on a piezoelectric bimorph. The deactivation and desensitization were recorded by 1- and 500-ms glutamate application, respectively, and analyzed by fitting with a single-exponential function, $A = A_0 \times \exp(-t/\tau) + C$, or a double-exponential function, $A = A_0 \times (f_1 \times \exp(-t/\tau_f) + f_2 \times \exp(-t/\tau_s)) + C$. In these functions, t is the time. The current amplitude (A) starts at A_0 and decays down to C. In our recording, the steady-state current C

was generally undetectable. f_1 and f_2 are the fractions of respective components as percentages ($f_1 + f_2 = 1$), and τ_f and τ_s are decay kinetics of fast and slow components. The weighted τ was calculated using the formula, weighted $\tau = f_1 \times \tau_f + f_2 \times \tau_s$. The recovery from desensitization was examined by pairs of 50-ms applications of 10 mM glutamate, with intervals ranging from 5 to 8000 ms. The recovery ratio was calculated via dividing the second peak amplitude by the first peak and analyzed by fitting with a single-exponential function, $f = (f_{max} - C) \times \exp(-t/\tau_{rec}) + C$, where t is the time; f_{max} is the maximal recovery; C is the nondesensitized steady-state fraction at the end of a 50-ms glutamate application; and τ_{rec} is the recovery constant.

Homology modeling

A three-dimensional model of Neto2CUB1 was made by homology modeling using Deepview software. The amino acid sequence of Neto2CUB1 was loaded into the workspace and searched the ExPDB database for appropriate templates. Cubilin (PDB entry 3KQ4) was chosen as an optimal template because of the high coverage rate (98%) and sequence identity (39%). The homologous sequence in cubilin was residues 234–346. The model was computed and built by the SWISS-MODEL server. This model and GluK2 NTD dimer structure (adapted from PDB entry 5KUF) were viewed and depicted using PyMOL software.

Statistical analysis

Data are presented as mean ± S.D. from three or more independent experiments. Statistical analyses were carried out using GraphPad Prism 7 software and analyzed using one-way ANOVA, two-way ANOVA, or unpaired t test if not otherwise stated. All p values < 0.05 were considered significant and labeled as follows: *, $p < 0.05$; **, $p < 0.01$; ***, $p < 0.001$.

Author contributions—Y.-J. L., G.-F. D., J.-H. S., D. W., and Y.-Y. S. data curation; Y.-J. L., G.-F. D., J.-H. S., and C. Y. formal analysis; Y.-J. L., G.-F. D., C. Y., Y.-Y. Z., G.-Q. C., and Y.-Y. S. methodology; D. W. and Y.-Y. Z. investigation; Y.-Y. Z., G.-Q. C., J. W., and W. Z. resources; Y.-Y. S., J. W., and Y. S. S. software; W. Z. and Y. S. S. supervision; W. Z. and Y. S. S. funding acquisition; Y. S. S. conceptualization; Y. S. S. writing-original draft; Y. S. S. writing-review and editing.

Acknowledgment—We thank Prof. Roger Nicoll (University of California, San Francisco) for critical comments on the manuscript.

References

1. Traynelis, S. F., Wollmuth, L. P., McBain, C. J., Menniti, F. S., Vance, K. M., Ogden, K. K., Hansen, K. B., Yuan, H., Myers, S. J., and Dingledine, R. (2010) Glutamate receptor ion channels: structure, regulation, and function. *Pharmacol. Rev.* **62,** 405–496 CrossRef Medline
2. Lerma, J., and Marques, J. M. (2013) Kainate receptors in health and disease. *Neuron* **80,** 292–311 CrossRef Medline
3. Schmitz, D., Mellor, J., and Nicoll, R. A. (2001) Presynaptic kainate receptor mediation of frequency facilitation at hippocampal mossy fiber synapses. *Science* **291,** 1972–1976 CrossRef Medline
4. Volk, L., Chiu, S. L., Sharma, K., and Huganir, R. L. (2015) Glutamate synapses in human cognitive disorders. *Annu. Rev. Neurosci.* **38,** 127–149 CrossRef Medline
5. Zhu, S., and Paoletti, P. (2015) Allosteric modulators of NMDA receptors: multiple sites and mechanisms. *Curr. Opin. Pharmacol.* **20,** 14–23 CrossRef Medline
6. Karakas, E., Regan, M. C., and Furukawa, H. (2015) Emerging structural insights into the function of ionotropic glutamate receptors. *Trends Biochem. Sci.* **40,** 328–337 CrossRef Medline
7. Möykkynen, T., Coleman, S. K., Semenov, A., and Keinänen, K. (2014) The N-terminal domain modulates α-amino-3-hydroxy-5-methyl-4-isoxazolepropionic acid (AMPA) receptor desensitization. *J. Biol. Chem.* **289,** 13197–13205 CrossRef Medline
8. Watson, J. F., Ho, H., and Greger, I. H. (2017) Synaptic transmission and plasticity require AMPA receptor anchoring via its N-terminal domain. *eLife* **6,** e23024 CrossRef Medline
9. Díaz-Alonso, J., Sun, Y. J., Granger, A. J., Levy, J. M., Blankenship, S. M., and Nicoll, R. A. (2017) Subunit-specific role for the amino-terminal domain of AMPA receptors in synaptic targeting. *Proc. Natl. Acad. Sci. U.S.A.* **114,** 7136–7141 CrossRef Medline
10. Plested, A. J., and Mayer, M. L. (2007) Structure and mechanism of kainate receptor modulation by anions. *Neuron* **53,** 829–841 CrossRef Medline
11. Sheng, N., Shi, Y. S., and Nicoll, R. A. (2017) Amino-terminal domains of kainate receptors determine the differential dependence on Neto auxiliary subunits for trafficking. *Proc. Natl. Acad. Sci. U.S.A.* **114,** 1159–1164 CrossRef Medline
12. Matsuda, K., Budisantoso, T., Mitakidis, N., Sugaya, Y., Miura, E., Kakegawa, W., Yamasaki, M., Konno, K., Uchigashima, M., Abe, M., Watanabe, I., Kano, M., Watanabe, M., Sakimura, K., Aricescu, A. R., and Yuzaki, M. (2016) Transsynaptic modulation of kainate receptor functions by C1q-like proteins. *Neuron* **90,** 752–767 CrossRef Medline
13. Jackson, A. C., and Nicoll, R. A. (2011) The expanding social network of ionotropic glutamate receptors: TARPs and other transmembrane auxiliary subunits. *Neuron* **70,** 178–199 CrossRef Medline
14. Howe, J. R. (2015) Modulation of non-NMDA receptor gating by auxiliary subunits. *J. Physiol.* **593,** 61–72 CrossRef Medline
15. Straub, C., and Tomita, S. (2012) The regulation of glutamate receptor trafficking and function by TARPs and other transmembrane auxiliary subunits. *Curr. Opin. Neurobiol.* **22,** 488–495 CrossRef Medline
16. Copits, B. A., and Swanson, G. T. (2012) Dancing partners at the synapse: auxiliary subunits that shape kainate receptor function. *Nat. Rev. Neurosci.* **13,** 675–686 CrossRef Medline
17. Wyeth, M. S., Pelkey, K. A., Yuan, X., Vargish, G., Johnston, A. D., Hunt, S., Fang, C., Abebe, D., Mahadevan, V., Fisahn, A., Salter, M. W., McInnes, R. R., Chittajallu, R., and McBain, C. J. (2017) Neto auxiliary subunits regulate interneuron somatodendritic and presynaptic kainate receptors to control network inhibition. *Cell Rep.* **20,** 2156–2168 CrossRef Medline
18. Orav, E., Atanasova, T., Shintyapina, A., Kesaf, S., Kokko, M., Partanen, J., Taira, T., and Lauri, S. E. (2017) NETO1 guides development of glutamatergic connectivity in the hippocampus by regulating axonal kainate receptors. *eNeuro* **4,** ENEURO.0048-17.2017 CrossRef Medline
19. Orav, E., Dowavic, I., Huupponen, J., Taira, T., and Lauri, S. E. (2019) NETO1 regulates postsynaptic kainate receptors in CA3 interneurons during circuit maturation. *Mol. Neurobiol.* 10.1007/s12035-019-1612-4 CrossRef Medline
20. Jack, A., Hamad, M. I. K., Gonda, S., Gralla, S., Pahl, S., Hollmann, M., and Wahle, P. (2019) Development of cortical pyramidal cell and interneuronal dendrites: a role for kainate receptor subunits and NETO1. *Mol. Neurobiol.* **56,** 4960–4979 CrossRef Medline
21. Vernon, C. G., and Swanson, G. T. (2017) Neto2 assembles with kainate receptors in DRG neurons during development and modulates neurite outgrowth in adult sensory neurons. *J. Neurosci.* **37,** 3352–3363 CrossRef Medline
22. Sargin, D. (2019) Heightened fear in the absence of the kainate receptor auxiliary subunit NETO2: implications for PTSD. *Neuropsychopharmacology* **44,** 1841–1842 CrossRef Medline
23. Mennesson, M., Rydgren, E., Lipina, T., Sokolowska, E., Kulesskaya, N., Morello, F., Ivakine, E., Voikar, V., Risbrough, V., Partanen, J., and Hovatta, I. (2019) Kainate receptor auxiliary subunit NETO2 is required for normal fear expression and extinction. *Neuropsychopharmacology* **44,** 1855–1866 CrossRef Medline

24. Stöhr, H., Berger, C., Fröhlich, S., and Weber, B. H. (2002) A novel gene encoding a putative transmembrane protein with two extracellular CUB domains and a low-density lipoprotein class A module: isolation of alternatively spliced isoforms in retina and brain. *Gene* **286,** 223–231 CrossRef Medline
25. Zhang, W., St-Gelais, F., Grabner, C. P., Trinidad, J. C., Sumioka, A., Morimoto-Tomita, M., Kim, K. S., Straub, C., Burlingame, A. L., Howe, J. R., and Tomita, S. (2009) A transmembrane accessory subunit that modulates kainate-type glutamate receptors. *Neuron* **61,** 385–396 CrossRef Medline
26. Fisher, J. L., and Mott, D. D. (2012) The auxiliary subunits Neto1 and Neto2 reduce voltage-dependent inhibition of recombinant kainate receptors. *J. Neurosci.* **32,** 12928–12933 CrossRef Medline
27. Tang, M., Pelkey, K. A., Ng, D., Ivakine, E., McBain, C. J., Salter, M. W., and McInnes, R. R. (2011) Neto1 is an auxiliary subunit of native synaptic kainate receptors. *J. Neurosci.* **31,** 10009–10018 CrossRef Medline
28. Sheng, N., Shi, Y. S., Lomash, R. M., Roche, K. W., and Nicoll, R. A. (2015) Neto auxiliary proteins control both the trafficking and biophysical properties of the kainate receptor GluK1. *eLife* **4,** e11682 CrossRef Medline
29. Duan, G. F., Ye, Y., Xu, S., Tao, W., Zhao, S., Jin, T., Nicoll, R. A., Shi, Y. S., and Sheng, N. (2018) Signal peptide represses GluK1 surface and synaptic trafficking through binding to amino-terminal domain. *Nat. Commun.* **9,** 4879 CrossRef Medline
30. Meyerson, J. R., Chittori, S., Merk, A., Rao, P., Han, T. H., Serpe, M., Mayer, M. L., and Subramaniam, S. (2016) Structural basis of kainate subtype glutamate receptor desensitization. *Nature* **537,** 567–571 CrossRef Medline
31. Copits, B. A., Robbins, J. S., Frausto, S., and Swanson, G. T. (2011) Synaptic targeting and functional modulation of GluK1 kainate receptors by the auxiliary neuropilin and tolloid-like (NETO) proteins. *J. Neurosci.* **31,** 7334–7340 CrossRef Medline
32. Fisher, J. L. (2015) The auxiliary subunits Neto1 and Neto2 have distinct, subunit-dependent effects at recombinant GluK1- and GluK2-containing kainate receptors. *Neuropharmacology* **99,** 471–480 CrossRef Medline
33. Fisher, J. L., and Mott, D. D. (2013) Modulation of homomeric and heteromeric kainate receptors by the auxiliary subunit Neto1. *J. Physiol.* **591,** 4711–4724 CrossRef Medline
34. Brown, P. M., Aurousseau, M. R., Musgaard, M., Biggin, P. C., and Bowie, D. (2016) Kainate receptor pore-forming and auxiliary subunits regulate channel block by a novel mechanism. *J. Physiol.* **594,** 1821–1840 CrossRef Medline
35. Fay, A. M., and Bowie, D. (2006) Concanavalin-A reports agonist-induced conformational changes in the intact GluR6 kainate receptor. *J. Physiol.* **572,** 201–213 CrossRef Medline
36. Straub, C., Zhang, W., and Howe, J. R. (2011) Neto2 modulation of kainate receptors with different subunit compositions. *J. Neurosci.* **31,** 8078–8082 CrossRef Medline
37. Sobolevsky, A. I. (2015) Structure and gating of tetrameric glutamate receptors. *J. Physiol.* **593,** 29–38 CrossRef Medline
38. Lu, H. W., Balmer, T. S., Romero, G. E., and Trussell, L. O. (2017) Slow AMPAR synaptic transmission is determined by Stargazin and glutamate transporters. *Neuron* **96,** 73–80.e4 CrossRef Medline
39. Twomey, E. C., Yelshanskaya, M. V., Grassucci, R. A., Frank, J., and Sobolevsky, A. I. (2017) Structural bases of desensitization in AMPA receptor-auxiliary subunit complexes. *Neuron* **94,** 569–580.e5 CrossRef Medline
40. Meyerson, J. R., Kumar, J., Chittori, S., Rao, P., Pierson, J., Bartesaghi, A., Mayer, M. L., and Subramaniam, S. (2014) Structural mechanism of glutamate receptor activation and desensitization. *Nature* **514,** 328–334 CrossRef Medline
41. Carbone, A. L., and Plested, A. J. (2012) Coupled control of desensitization and gating by the ligand binding domain of glutamate receptors. *Neuron* **74,** 845–857 CrossRef Medline
42. Schauder, D. M., Kuybeda, O., Zhang, J., Klymko, K., Bartesaghi, A., Borgnia, M. J., Mayer, M. L., and Subramaniam, S. (2013) Glutamate receptor desensitization is mediated by changes in quaternary structure of the ligand binding domain. *Proc. Natl. Acad. Sci. U.S.A.* **110,** 5921–5926 CrossRef Medline
43. Griffith, T. N., and Swanson, G. T. (2015) Identification of critical functional determinants of kainate receptor modulation by auxiliary protein Neto2. *J. Physiol.* **593,** 4815–4833 CrossRef Medline
44. He, X. Y., Li, Y. J., Kalyanaraman, C., Qiu, L. L., Chen, C., Xiao, Q., Liu, W. X., Zhang, W., Yang, J. J., Chen, G., Jacobson, M. P., and Shi, Y. S. (2016) GluA1 signal peptide determines the spatial assembly of heteromeric AMPA receptors. *Proc. Natl. Acad. Sci. U.S.A.* **113,** E5645–E5654 CrossRef Medline